Available online at www.sciencedirect.com

ScienceDirect

Geochimica et Cosmochimica Acta 71 (2007) 1674–1688

Geochimica et Cosmochimica Acta

www.elsevier.com/locate/gca

Geochemistry and origin of ferruginous nodules in weathered granodioritic gneisses, Mysore Plateau, Southern India

Jayant K. Tripathi *, V. Rajamani

National Facility for Geochemical Research, School of Environmental Sciences, Jawaharlal Nehru University, New Delhi 110067, India

Received 23 November 2005; accepted in revised form 3 January 2007; available online 10 January 2007

Abstract

Fe-nodules occur within saprolites formed from weathering of granodioritic gneisses in the rain-shadow region of the Mysore Plateau adjacent to the Sahyadri Mountains in Southern India. These nodules and their host saprolites were studied for their geochemistry, including chemical speciation, to understand nodule formation and chemical redistribution processes during rock weathering. From their mode of occurrence, and mineralogical and geochemical data, we infer that the nodules originated by a two-stage process in which the initial extensive weathering of gneisses likely facilitated subsequent ferrolysis weathering and nodule formation. Nodules originated by precipitation of goethite, hematite and gibbsite along with several amorphous phases within the matrix of weathered gneisses. This is possible only under hydromorphic conditions, suggesting that parts of the plateau must have gone through a humid phase prior to the present aridity. In the saprolites, Al, Fe, and Ti become enriched because of the removal of Si, Ca, Na, and K. However within the nodule, Fe, Ti, Cr, and Ni are deposited after their chemical transport from the saprolite. Titanium, known for its immobile nature, was also mobilized and concentrated under the conditions of nodule formation. The most important elements in the nodule constitution are Fe, Al, Ti, and Mn, each having both crystalline and amorphous phases. Fe–Ti and Mn oxyhydroxides grain coatings in the saprolites and discrete amorphous Mn and Ti phases in the nodules seem to have scavenged trace elements from the weathering profile. REE were mobilized during weathering and nodule genesis in which Ce and Ti show a strong geochemical coherence. The enrichment of only HREE in saprolite, and both HREE and LREE with significant Ce in the nodule, indicate the control of evolving secondary minerals in the REE redistribution during rock weathering. Strong enrichment of Ce in the weathering profile and in nodules has important implications to the REE chemistry of river waters.

1. INTRODUCTION

Fe–Mn nodules occur on the ocean floor at all latitudes (Crerar and Barns, 1974); continental soil nodules, however, are less abundant and only occur in the fine-textured soils of warm humid areas. The Fe content of these soil nodules has been shown to increase with mean annual precipitation (Stiles et al., 2001). There has been considerable interest and discussion on the origins of oceanic and continental nodules based on their geochemistry. Oceanic nodules are thought to form by adsorption and catalytic oxidation of Fe and Mn at nucleating surfaces, and grow through autocatalysis (Palumbo et al., 2001). Marine bacteria also seem to play an important role in accelerating the rate of precipitation and nodule formation (Crerar and Barns, 1974). In soils, seasonal changes in soil redox potential and pH are known to cause precipitation of nodule minerals in soil/sediment pore spaces (Burns and Burns, 1975; Palumbo et al., 2001 and references therein). Here again, precipitation of nodule minerals is thought to be microbially mediated (Spilde et al., 2002). Repetitive dissolution of Fe and Mn during wet periods and precipitation during dry periods often produces concentric nodule layering due to seasonal growth (Manceau et al., 2003). Nahon (1991) suggested that epigenetic replacement of kaolinite

---

* Corresponding author. Present address: Wadia Institute of Himalayan Geology, 33, GMS Road, Dehradun 248001, India.
E-mail address: jktrip@yahoo.com (J.K. Tripathi).

0016-7037/$ - see front matter © 2007 Elsevier Ltd. All rights reserved.
doi:10.1016/j.gca.2007.01.001

crystals by aluminous hematite produces ferruginuous nodules within kaolinitic plasma. Gasparatos et al. (2004) reported that Fe-rich nodules containing primary silicate minerals indicate precipitation of Fe phases in the soil pores. Soil ferruginous nodules, because they commonly form under humid climatic conditions, are considered to be palaeoclimate indicators (Stiles et al., 2001; Yapp, 2001). Because of their importance in palaeoclimate studies and biogeochemical processes, these continental nodules need to be better studied in different geographic and geologic settings to understand their formation and genetic significance.

The chemistry of the rare earth elements (REE) in oceanic nodules has been used to understand nodule genesis as well as the composition of palaeo-seawater (Piper, 1974; Elderfield et al., 1981; Pattan et al., 2001). The REE are useful in such studies because they are expected to behave coherently unless the physical conditions of the natural environment and/or the formation of certain minerals fractionate some elements selectively. For example, Ce^{3+} can oxidize to Ce^{4+} in oxygenated water and be preferentially removed from solution by Fe–Mn minerals, producing a negative Ce anomaly in ocean water (Goldberg et al., 1963; Byrne and Sholkovitz, 1996; Bau et al., 1996). The REE composition of planktonic and benthic foraminifera is controlled by the REE distribution in the water column, enabling use of REE composition in foraminifera as a useful proxy for paleoceanographic and climate change (Haley et al., 2005). Unlike certain primary minerals in a rock systems, such as garnet for heavy REE or epidote for light REE, which can fractionate the REE, secondary minerals are not particularly known to produce strong REE fractionation behavior. Nevertheless, certain 2:1 clay minerals formed during rock weathering are thought to preferentially incorporate HREE (Nesbitt, 1979). Dutta et al. (2005) found a positive correlation of REE with Fe content of the nodules of the Indian Ocean. It has been shown (Haley et al., 2004) that the REE chemistry of pore waters of marine sediments was strongly influenced by Fe-oxides (for middle REE), organic carbon (for heavy REE) and discrete Ce-oxide phases (for Ce-anomaly). Therefore, the REE geochemistry of soil nodules could potentially be useful in deciphering the environmental conditions of their formation. However, this aspect of REE behavior has not been studied for soil nodules. In general, the mechanism of mobilizing, transporting and precipitating various elements in the Fe nodules formed during rock weathering is not well understood.

In the Mysore Plateau, Southern India, the weathered ganodioritic gneisses of Archean age show widespread development of ferruginous nodules within saprolites, especially in the catchment area of the Kaveri River (Fig. 1). Although geomorphic features and soil characteristics have been reported from this region (Bourgeon, 2001; Gunnel, 2001), no serious studies have been carried out to understand the nature and extent of weathering of various lithologies here, and the development of lateritic caps, ferricrete, and Fe nodules. As a part of our major effort to study rock weathering and sediment production processes in the Kaveri River Basin using a geochemical approach, we studied the mineralogical and geochemical characteristics of Fe nodules developed within saprolites of granodiorite gneisses. In addition to promoting a better understanding of soil nodule formation, our study also illuminates the interesting weathering-behavior of elements such as Ti and Ce and its implications for sediment geochemistry and application to paleoclimate and provenance.

2. GEOLOGY AND CLIMATE OF THE REGION

The Mysore Plateau (altitude 900–1200 m) with its mountainous and high relief region to the west (Sahyadris: altitude 900–1900 m) constitutes the catchment area of the Kaveri River, one of the major rivers of Southern India (Fig. 1). The Sahyadri Mountains rise precipitously from the narrow western coastal region, with peaks reaching up to 2700 m in the southern parts. The Kaveri catchment region includes dominantly granodioritic and migmatitic gneissic rocks of Archean age (>2500 Ma) with amphibolitic enclaves in the northern part and their granulitic equivalents in the southern part of the plateau. A 100 km wide metamorphic transition zone separates the two parts. North of this zone, the gneissic rocks with included supracrustal belts (schist belts) are metamorphosed to grades lower than amphibolite facies. South of the transition zone, both gneissic and supracrustal rocks are commonly metamorphosed to granulite grade resulting in the formation of charnockite, pyroxene granulite and high grade amphibolite assemblages (Fig. 1). These rock types are intensively weathered and lateritized in the humid western parts of the catchment area. In the semi-arid regions to the east (a rain-shadow effect associated with prevailing southwesterly monsoonal winds) rocks have undergone much less chemical weathering but show ferruginized regolith and thin lateritic caps. Generally, these laterites occur at elevations between 800 and 1000 m above sea level (Radhakrishna, 1952).

The study area near Belur (Fig. 1) is located on the western part of the Dharwar Craton where the ages of the country gneisses are known to be 3300–3000 Ma (Radhakrishna and Vaidyanadhan, 1997). These Peninsular Gneisses in places are migmatitic, as in the present study area, with leucosomes (granitic), melanosomes (biotite rich), abundant quartz veins and amphibolitic enclaves. In the present study area, the weathering profiles are developed over the granitic leucosome with enclaves of biotite gneiss and quartz veins.

The nature and lithological make up of the Belur profile, a road cut section, are presented here using lithologs (Fig. 2). Thick saprolites after the gneisses are overlain by locally reworked and differentiated regolith. The saprolites in the lower part of the profile are bleached and white, whereas the upper part is reddish and ferruginous. The upper part of the saprolite profile contains Fe-nodules of varying sizes, up to about 1 cm diameter. The nodules are also present along with coarser quartz pebbles in the overlying gravel bed, likely concentrated by the reworking of regolith.

The biotite gneisses, protected by quartz veins (Fig. 2C) are relatively less altered (saprolithic). The quartz veins are highly fractured and supplied quartz pebbles after erosion.

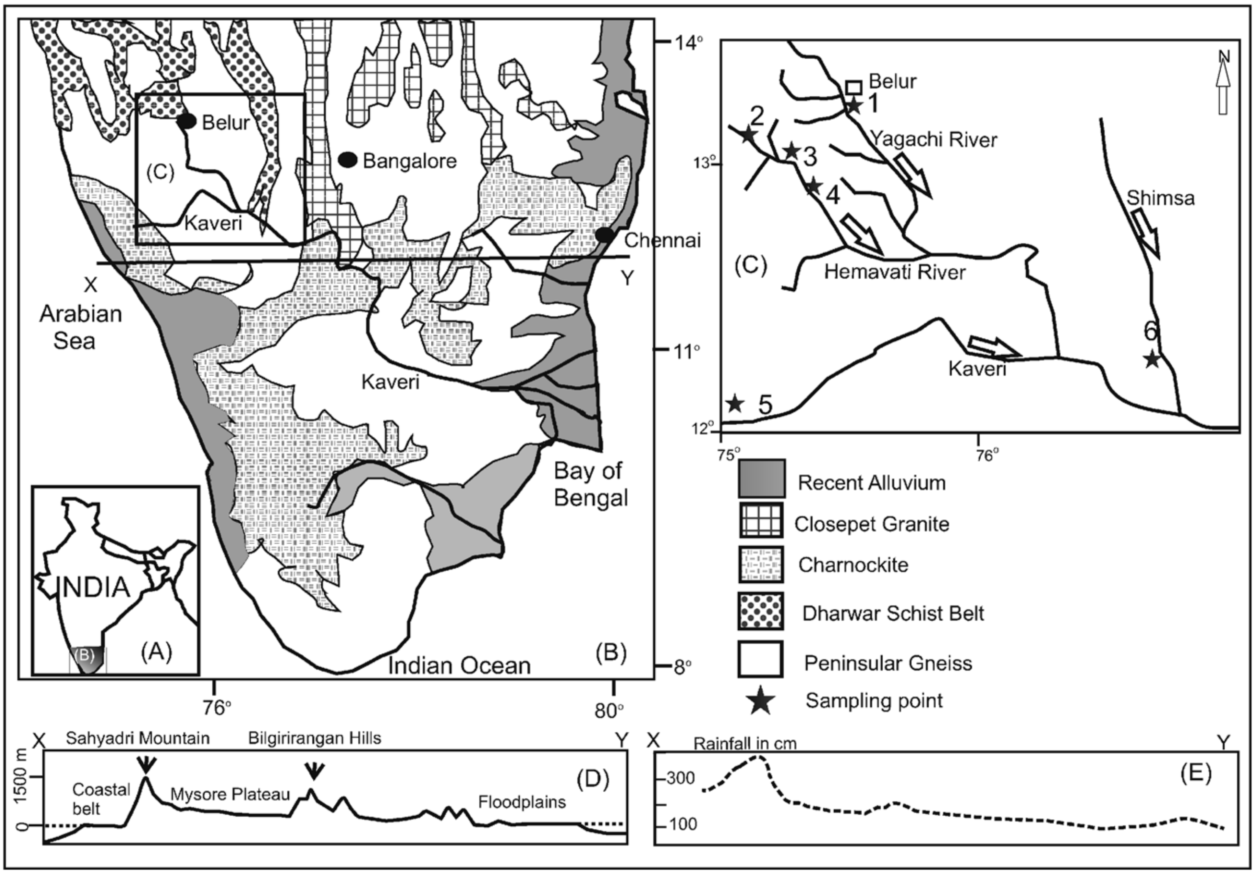

Fig. 1. Geological map of Southern India showing the study area near Belur in the Peninsular Gneisses of the Western Dharwar Craton (B). The sampling points are shown in (C). A generalized topographic profile across X–Y is shown in (D) (after Babu, 1975). Annual rainfall distribution is shown in (E) (modified after Gunnel, 1988).

The regolith mainly contains quartz pebbles, Fe-nodules, amphibolite boulders, and silty sediments. Local reworking differentiated these materials into a quartz gravel bed, a Fe-nodule bed and organic-rich silty sediments with occasional quartz pebbles. Pebbles or fragments of bedrock gneisses are typically absent in the regolith. Generally, the weathered gneisses are overlain by variably thick quartz gravel bed (~0.5–1 m). This bed contains mainly sub-rounded quartz pebbles, sometimes imbricated and mixed with fine sandy material and Fe nodules. Occasionally, amphibolite boulders also occur in this bed. This bed is overlain by silty and poorly sorted organic-rich sediments. The complete sequence containing gravel beds and sediments (Fig. 2A) is developed in local depressions, whereas in places weathered gneisses are directly overlain by organic rich sediments (Fig. 2B). Less weathered biotite gneisses (saproliths) protected by quartz veins and occurring in association with saprolites are shown in Fig. 2C. In some places, where saprolite is directly overlain by silty sediments, calcrete nodules (rhizolithic) occur in the weathered and bleached gneisses (Fig. 2B) indicating evapotranspiration and CO_2 exchange processes through soil, in the prevailing semi arid climate. In places, below the sediments, the gravels are also coated with secondary carbonates. The fresh unweathered gneisses can be seen only along a deep, nearby canal cutting at a depth of more than 7 m, indicating the occurrence of fresh rock at a depth of around 4 m below the exposed weathering profile.

The study area experiences a semi-arid to sub-humid tropical climate and receives an annual rainfall of about 100 cm, mostly between June and August from the SW monsoon. The mean annual temperature of the Kaveri catchment is 25 °C, although in summer (March–May) the maximum temperature may reach 43 °C. The precipitation in the basin decreases from west to east (Fig. 1E). The present study area in the basin, Belur in Hassan District, is a semi arid region with yearly precipitation around 80 cm, whereas around 100 km to the west, the Sahyadri mountainous region receives an average rainfall in excess of 400 cm.

On the basis of studies of peatbogs from the nearby Nilgiri mountains (200 km south), Caner and Bourgeon (2001) suggested that the period from 30 to 18 K was relatively drier than the present; between 18 and 10 K there was a shift toward a more humid climate and expansion of forests, and the period from 10 K to present was characterized by alternating wetter and drier periods.

3. MATERIALS AND METHODS

To understand the widespread development of Fe nodules in the region, four samples of saprolites (C1–C4) were

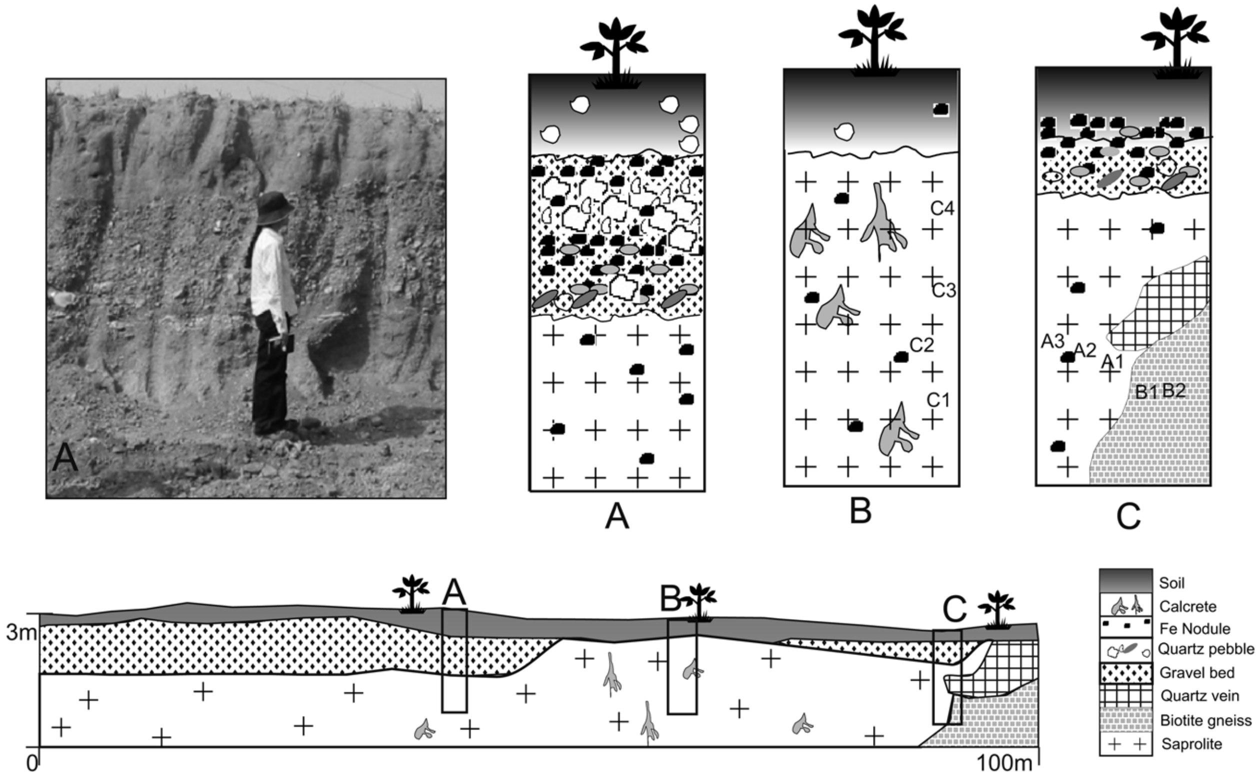

Fig. 2. Belur section containing thick saprolites after the gneisses, which are overlain by differentiated regolith. The complete sequence containing gravel beds and soils (A) are developed in local depressions, whereas, occasionally weathered gneisses are directly overlain by organic rich sediments (B). In some places, where saprolite is directly overlain by soils, calcrete nodules (rhizolithic) occur in the weathered and bleached gneisses (B). Less-weathered biotite gneisses (saprolith) protected by quartz veins occur in association with saprolites and overlain by gravel beds and sediments (C).

collected from the Belur section B (Fig. 2) and three more samples (A1, A2, and A3) from near the biotite gneiss pockets (samples B1 and B2) from section C (Fig. 2). Because no fresh rocks are exposed directly underneath the profile, a representative sample of the bed rock (GN1) was collected from a nearby canal cutting. Care was taken to select rock that was texturally and structurally very similar to the bedrock of the sampling profile. Granodiorite gneisses with mineralogies and chemistries (including rare earth elements) similar to sample GN1 have been reported from this area (Bhaskar Rao et al., 1991; Rama Rao and Divakara Rao, 1994). Samples of Fe-nodules (N1 and N2) developed within the saprolites of section B and C were plucked out of the profiles. Similarly, nodule samples N4 were collected from saprolites at sampling point-3. In addition to these nodule samples, we had also collected nodules from the channel sands of the Hemavati and Shimsa (tributaries) and the Kaveri River from locations 2 (N6), 3 (N5), 5 (N7) and 6 (N8) (Fig. 1C). Nodule sample N3 was plucked out of a ferricretised sediment profile deposited on weathered gneisses (sampling point-4).

Four kilograms of each sample of saprolites/rocks and 500 g of nodules were collected and crushed to 250 μm. Out of the total 4 kg sample processed (500 g for nodules), about 200 g of each sample was ground to 75 μm size for geochemical and XRD mineral analysis. Mineralogy of weathered samples and nodules was studied using a Philips X'pert powder diffractometer with an accelerating voltage of 50 kV, a tube current of 40 mA and a scanning speed of 2° 2θ per minute. Minerals were identified using Philips X'pert HighScore (version 1) software program.

All the samples shown in Table 1 are digested in open beakers (teflon) using a combination of $HF + HNO_3 + HClO_4$ for analysis of major and trace elements. The alkali hydroxide and peroxide fusion method was followed for the digestion of samples for REE determination. REE separation and pre-concentration were performed with a cation exchange resin (Dowex 50, 100–200 mesh size, H form; for details of column chemistry see Tripathi and Rajamani, 1999). The REE data is shown in Table 2. Silica gel, which separated from the REE bearing solution after the alkali hydroxide and peroxide fusion, was used for gravimetric analysis of silica. Speciation analysis of the nodules was performed by a method modified after Leleyter and Probst (1999). To minimize the loss of material during speciation steps, the following procedure was adopted: (1) a polypropylene centrifuge tube (60 ml) was used for 1 g of powdered sample (<75 μm size), (2) subsequent to a prescribed temperature and time of agitation on the shaker that allowed complete reaction between the sample and the reagents during each step, the tube was centrifuged (7000 rpm) and the supernatant was filtered through 0.45 μm filter paper (Whatman). The residue on the filter paper was returned to the residue remaining in the tube

Table 1
Major (%) and trace (ppm) elements chemistry of saprolites after granodioritic gneisses (A1–A3, and C1–C4), biotite rich gneisses (B1 and B2), parent granodioritic gneiss (GN1) and Fe-nodules (N1–N8)

	A1	A2	A3	B1	B2	C1	C2	C3	C4	N1	N2	N3	N4	N5	N6	N7	N8	GN1
SiO_2	62.6	63.2	56.3	39.5	38.1	68.5	65.9	62.9	59.8	20.4	17.8	35.0	27.5	28.5	43.8	33.5	35.3	71.2
TiO_2	0.3	0.4	0.6	1.7	1.6	0.2	0.3	0.3	0.4	1.2	1.6	0.3	0.7	0.6	0.5	1.3	0.3	0.1
Al_2O_3	20.5	20.3	20.9	18.2	23.4	20.3	23.1	25.0	26.3	20.3	16.7	8.3	17.2	16.7	13.0	15.7	9.7	12.1
FeO(T)	2.0	4.5	8.5	17.9	19.7	2.1	3.0	4.1	5.3	42.2	48.3	44.1	38.6	37.0	28.4	33.8	26.5	0.9
MnO	bdl	0.0	0.0	0.2	0.1	0.0	0.0	0.0	0.0	0.2	bdl	0.0	0.4	0.3	0.5	0.3	2.3	0.0
MgO	0.0	0.1	0.1	7.6	1.0	0.2	0.1	0.2	0.2	0.0	bdl	0.0	0.1	0.1	0.2	0.3	0.6	0.1
CaO	0.1	0.1	0.1	0.2	0.1	bdl	bdl	bdl	bdl	bdl	0.1	bdl	bdl	0.0	0.3	0.3	7.2	1.4
Na_2O	0.2	0.1	0.2	0.2	0.2	0.0	0.0	0.0	0.1	0.8	0.2	0.3	0.8	0.8	0.4	0.2	0.4	5.8
K_2O	2.1	0.5	0.5	4.8	0.4	2.3	1.0	1.0	0.8	0.0	0.0	0.2	0.2	0.2	0.6	0.1	0.6	2.2
P_2O_5	0.01	0.01	0.02	0.03	0.03	bdl	bdl	bdl	0.02	0.10	0.10	0.21	0.24	bdl	0.24	0.33	0.10	bdl
LOI	11.4	10.6	11.5	9.8	14.6	6.3	6.5	6.4	7.3	14.9	16.2	10.9	13.5	14.5	11.8	14.3	16.7	2.5
Total	99.1	99.8	98.7	100.0	99.1	100.0	100.0	100.0	100.2	100.2	100.9	99.4	99.3	98.9	99.6	100.1	99.7	96.3
Trace elements (ppm)																		
Ba	587.8	167.5	153.6	335.1	145.5	550.8	252.4	217.0	11.5	163.2	105.6	49.5	17.7		185.8	30.1	2118.9	708.9
Co	4.2	7.4	9.3	42.5	21.1	bdl	bdl	bdl	8.3	56.2	61.9	23.7	76.4		119.1	72.8	96.3	
Cr	108.0	209.4	409.7	676.3	649.5	69.6	109.2	121.8	141.2	3308.9	4090.2	1171.5	2871.4		591.1	3732.0	665.4	7.2
Cu	61.4	46.5	132.5	39.8	65.7	34.6	103.0	56.0	48.5	207.1	258.2	71.7	112.8		54.4	227.5	114.7	
Ni	58.4	86.9	114.7	242.7	168.8	135.6	51.2	59.4	85.1	255.1	355.8	104.4	281.4		113.4	217.2	243.7	bdl
Sr	55.8	13.6	15.1	8.6	9.3	60.8	9.0	8.8	20.1	4.4	4.7	6.6	7.4		35.2	11.5	157.7	575.8
V	32.8	75.3	134.3	292.6	302.2	49.2	71.2	84.0	83.0	659.7	951.8	1028.2	599.2		244.5	456.8	343.2	
Zn	82.3	44.1	81.5	516.2	169.0	bdl	bdl	95.4	46.2	86.6	76.7	90.8	116.0		107.7	153.1	58.9	

Table 2
Rare earth elements (ppm) chemistry of saprolites, parent granodioritic gneiss (GN1) and Fe-nodules

	A1	A2	A3	B1	B2	C1	C2	C3	C4	N1	N2	N3	N4	N5	N6	N7	N8	GN1
La	4.6	5.9	5.5	31.8	20.4	3.5	8.0	7.8	6.2	11.1	9.2	43.8	12.7	11.4	25.4	39.0	57.6	9.6
Ce	8.5	17.0	15.3	96.0	117.8	10.3	15.3	26.2	19.8	65.7	80.8	372.0	71.6	81.4	125.2	116.6	243.4	18.4
Nd	3.9	5.7	4.5	35.6	19.0	3.8	7.8	6.4	4.6	13.7	8.9	35.2	13.7	11.6	24.0	46.0	43.6	6.8
Sm	0.9	1.1	0.9	6.3	4.0	1.0	1.6	1.6	1.2	3.2	2.0	9.2	3.2	3.2	5.4	9.6	9.2	1.6
Eu	0.3	0.4	0.3	2.2	1.3	0.3	0.5	0.4	0.4	1.0	0.6	1.2	0.9	1.2	1.2	1.4	2.0	0.6
Gd	0.9	1.4	0.9	6.5	4.3	1.0	1.8	1.4	1.0	3.2	1.8	7.8	3.1	3.2	5.2	8.0	8.4	1.0
Dy	1.0	1.6	1.1	4.8	3.9	1.0	1.7	1.6	1.2	2.8	1.7	6.6	2.7	3.0	4.6	6.0	6.4	0.8
Er	0.6	1.0	0.6	2.3	2.1	0.6	1.0	1.0	0.8	1.4	0.8	3.4	1.3	1.4	2.4	3.4	3.4	0.4
Yb	0.6	1.1	0.7	1.8	2.0	0.8	1.1	1.0	0.8	1.6	0.7	4.2	1.8	1.8	2.6	4.2	3.8	0.2

to minimize the loss. The supernatant, meant for speciation analysis, was stored in a 20 ml polypropylene bottle at 4 °C. The residue in the tube was washed with 10 ml of ultrapure water, centrifuged, and the supernatant rinsing water was removed before drying (at 40 °C) and entering into the next step. For sequential leaching, the following steps were performed using different reagents and procedures: (1) water soluble extraction (with 10 ml distilled water; 30 min reaction time at 20 °C), (2) exchangeable ion extraction (with 10 ml of 1 M magnesium nitrate, 2 h reaction time at 20 °C), (3) amorphous oxides extraction (with 10 ml of 0.2 M ammonium oxalate–0.2 M oxalic acid; 4 h in the dark at 20 °C) and (4) crystalline iron oxide extraction (with 10 ml of 0.2 M ammonium oxalate–0.2 M oxalic acid–0.1 M ascorbic acid; 30 min reaction time at 80 °C).

All the elements were analyzed by Jobin Yvon ICP-OES (ULTIMA 2). The precision and accuracy of analyses for major and trace elements including REE were monitored using USGS rock standards (BHVO, STM, and RGM), as well as in house rock and sediment standards, and are to be better than 5% and 2%, respectively. Ce and Nd have a precision of 5–10% for samples low in LREE content (<10 times chondrite). Multielemental standards, prepared from pure REE metal standards (Johnson Mathey, USA) were used for instrument calibration. The efficacy of our sample dissolution procedures was checked by analyzing different aliquots of the same sample wherever possible.

4. RESULTS AND DISCUSSION

4.1. Mineralogy of weathering profile and nodules

The X-ray diffraction data and petrographic observation of a thin section show that the unweathered gneissic parent rock is mainly composed of quartz, alkali feldspar, muscovite, and biotite. Illite and kaolinite appear in the less weathered saprolite samples (A1 and C1). Goethite, gibbsite, chlorite, and vermiculite are present in the extensively weathered samples. Relatively less weathered biotite gneiss is composed of biotite, chlorite and feldspar, whereas hematite, kaolinite, and goethite appear in more weathered samples.

The nodules are mainly composed of goethite, hematite, and kaolinite. The presence of opal/silica (in N1, N2, and N6), gibbsite (in N1, N3, and N4) and anatase and titania (TiO_2) in the nodules were also shown in the X-ray diffraction patterns. Other important phases in the nodules and saprolites, which were not discernible by the X-ray method because of their amorphous form, are identified by speciation and statistical analysis of elemental distribution data.

4.2. Major element chemistry

It is very important to understand the mobilization and redistribution of different elements from the rocks during weathering and formation of the nodules. The A–CN–K and A–CNK–FM systematics and the Chemical Index of Alteration (CIA) are useful to understand the weathering trends of gneisses and redistribution of elements that are relatively immobile (Al and Fe) and mobile (Ca, Na, K, and

Mg). To quantify the extent of weathering (Chemical Index of Alteration) and to plot in the A–CN–K and A–CNK–FM diagrams, molar proportions of Al_2O_3 (A), CaO (C), Na_2O (N), K_2O (K), FeO (F), and MgO (M) were calculated from the chemical data (Nesbitt and Young, 1989). The Chemical Index of Alteration (CIA) is defined as:

$$\mathrm{CIA} = (Al_2O_3/(Al_2O_3 + CaO^* + Na_2O + K_2O)) \times 100,$$

where CaO^* represents the calcium in the silicate fraction only. In the absence of CO_2 data, correction for CaO in calcite is difficult. Therefore, in the samples where the CaO molecular proportion is greater than the molecular proportion of Na_2O, the CaO is assumed to be equal to Na_2O (McLennan, 1993).

Before we discuss the behavior of elements during weathering and formation of Fe-nodules from bedrock granodioritic gneisses, we need to evaluate the exact geochemical nature of the underlying bedrock. A sample of unweathered rock could not be obtained from the studied profile because of the high intensity of weathering. However the saprolite sample C1, deepest in the profile, shows relict gneissic structure and mineralogy similar to the fresh sample of the gneiss GN1 collected from the nearby canal cutting. Earlier studies of the geochemistry of these granodioritic rocks from this area did show a large variation, particularly in the abundance of trace elements. Rocks with compositions including REE chemistry similar to the chosen bedrock sample GN1 were also reported from this area (Bhaskar Rao et al., 1991). These considerations, and the complementary nature of biotite-gneiss samples to the GN1 sample in their chemistry, suggest that sample GN1 is likely to be representative of the bed rock below the profile. All the analyzed samples of the saprolites are also internally consistent with this "representative" bedrock sample, GN1. We do realize that large variations, particularly in trace element abundance, are a rule in granitic rocks. Therefore, we need to exercise a great deal of caution in interpreting our chemical data.

In the A–CN–K diagrams (Fig. 3), we observe that weathering of gneisses from parent rock GN1 proceeded along the CN–A line and resulted in significant loss of CaO and Na_2O. With continued weathering, the weathering trend moved towards the 'A' corner along the 'A–K' join, indicating subsequent loss of 'K_2O'. Highly weathered samples plot at the 'A' corner. The nodules in the A–CN–K diagram (Fig. 3) plot near the 'A' corner but show some 'CN' component in them. How this 'CN' (Ca and Na) component can occur in the nodules developed within the saprolite needs explanation. The CIAs or A–CN–K plot of the nodules actually represent entrapped aluminosilicate minerals within the matrix of the nodules and also elements scavenged by the Fe–Mn phases of the nodules. In the A–CNK–FM diagram (Fig. 3), weathering of gneisses first shows the loss of CNK with a relative enrichment of 'A' component along the 'A–CNK' line. With further weathering we find enrichment of 'FM' component over 'A' component. Samples of biotite gneiss plot at higher 'FM' because of their higher Fe contents. Nodules plotting near the extreme end of the 'FM' corner in the A–CNK–FM diagram suggest enrichment of iron over Al in the saprolite, which plays an important role in making the nodules. This trend of weathering of gneisses as well as the plots of nodules in the high 'FM' zone provide clues to the mechanism of formation of the nodules during rock weathering. Initial weathering of gneisses results in enrichment of ferruginous material in the saprolite; and later local accretion of ferruginous material within the saprolite zone resulted in nodule formation.

It has been suggested that fine porosity developed in rocks due to weathering, and formation of clay minerals in the highly weathered zones favors precipitation of goethite (Nahon, 1991). Schwertmann and Murad (1983) suggested that hematite or its hydrated precursor (ferryhydrite) is precipitated in a porous rock instead of goethite. During the mineralisation of hematite/ferryhydrite/goethite, the aluminosilicate clay minerals could have further weathered to produce gibbsite (from kaolinite). XRD data show the presence of goethite, gibbsite, and kaolinite minerals in the nodules. The reactions involved in the weathering of kaolinite during nodule formation (modified after Nahon, 1991) and mineralisation of ferryhydrite/goethite/hematite and gibbsite are shown below.

$$Fe^{2+} = Fe^{3+} + e^- \tag{1}$$

$$Fe^{3+} + 2H_2O = FeOOH + 3H^+ \tag{2.a}$$

$$2Fe^{3+} + 3H_2O = Fe_2O_3 + 6H^+ \tag{2.b}$$

$$Si_2Al_2O_5(OH)_4 + 6H^+ = 2Al^{3+} + 2H_4SiO_4 + H_2O \tag{3}$$

$$Al^{3+} + 3H_2O = Al(OH)_3 + 3H^+ \tag{4}$$

It is interesting to note that these reactions involving mineral formation in nodules can occur only in hydromorphic conditions (Stiles et al., 2001). However, the study area presently experiences a semiarid to arid climate. This indicates that this region must have gone through a very humid climate with a high mean annual precipitation prior to the present arid conditions. The area is less than 100 km away from the humid tropical rain forests of Sahyadris (average rainfall 400 cm). The geodynamics of the region, which has altered the landscape of the plateau, must have also locally altered the climate of the study area in Southern India (see Radhakrishna, 1993).

The major element chemistry and A–CN–K and A–CNK–FM systematics for the saprolites show a depletion of silica, Na, K, and Ca relative to the parent rock, with accompanying enrichment of Al, Fe and Ti. Among the trace elements analyzed, Ba and Sr show a notable depletion whereas Cr and V are residually enriched in saprolites. Other analyzed elements do not show any regular trend. In response to chemical denudation of various elements from the weathering profile and their reprecipitation as nodules, the nodule aggregates show an accumulation of Fe, Ti, Cr, Ni, and V. Although Al concentrations are lower in the nodules relative to the saprolites and the parent rock, Al rich minerals (kaolinite and gibbsite) and high CIA values were encountered for the nodules. Ti and Al are reported to be relatively immobile elements in sedimentary processes (Young and Nesbitt, 1998) and, therefore, have been used to quantify the extent of weathering (Nesbitt, 1979; Middelburg et al., 1988; Young and Nesbitt, 1998; Sharma and Rajamani, 2000, 2001) and identify provenance (Maynord,

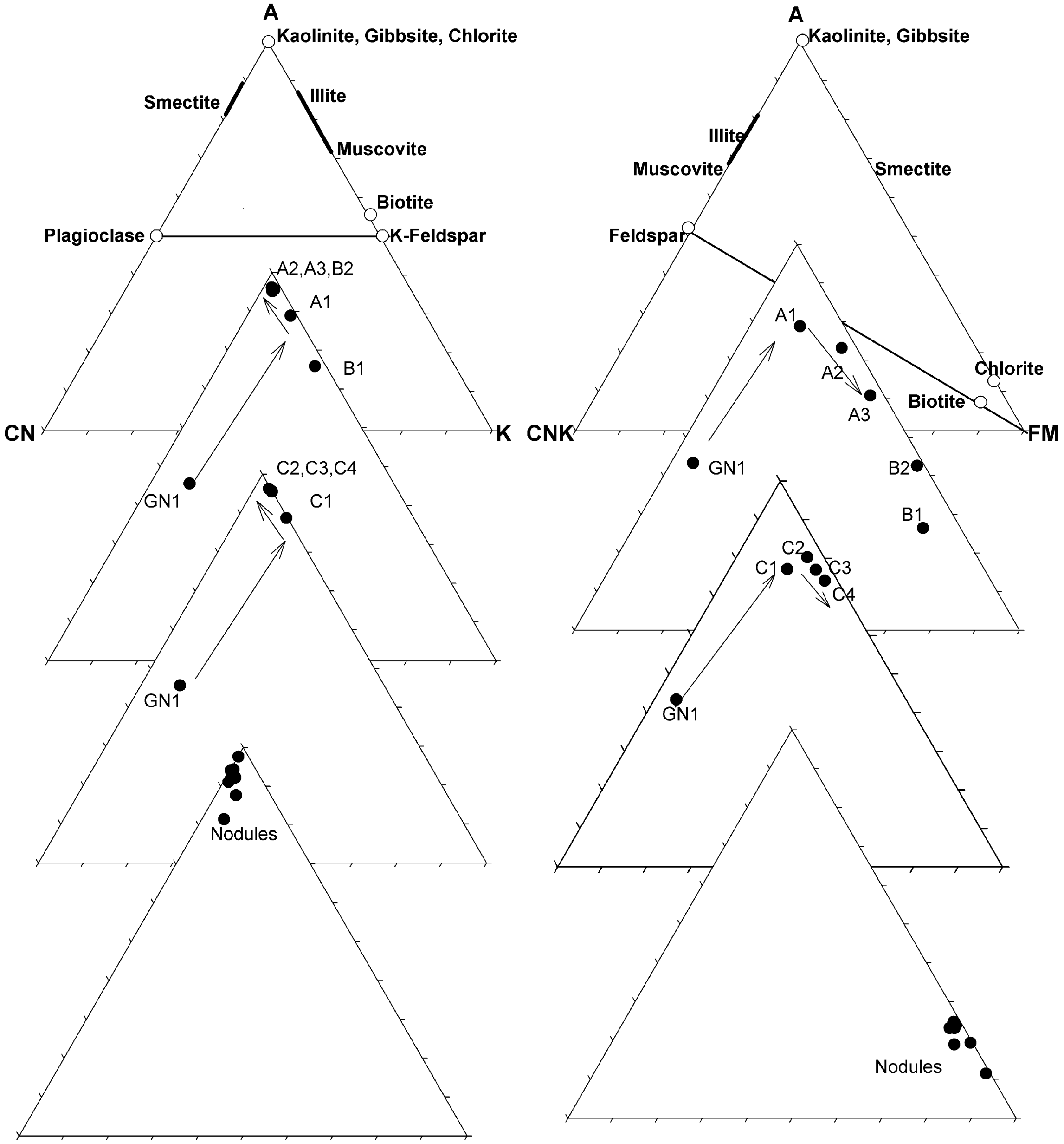

Fig. 3. A–CN–K (Al_2O_3–CaO + Na_2O–K_2O) and A–CNK–FM (Al_2O_3–CaO + Na_2O + K_2O–FeO + MgO) diagrams showing common primary and secondary minerals and weathering trends from gneisses to saprolites and nodules. In the A–CN–K diagram, gneisses weather in a trend parallel to the 'A–CN' line showing a significant loss of Ca and Na. With continued weathering, the weathering proceeds towards the 'A' corner along the 'A–K' join indicating subsequent loss of 'K'. Highly weathered samples plot at the 'A' corner. In the A–CNK–FM diagram, weathering of gneisses first shows the loss of CNK with a relative enrichment of 'A' component along the 'A–CNK' line. Further weathering causes enrichment of 'FM' component over the 'A' component. The nodules plot in A–CN–K diagram towards 'A' corner but show some 'CN' (Ca + Na) component with them. Samples of biotite gneiss plot closer to the 'FM' apex because of their higher Fe content. Nodules plotting near the extreme end of the 'FM' corner in the A–CNK–FM diagram suggest enrichment of iron over Al in the saprolite, which plays an important role in making the nodules.

1992; Haug et al., 2003). However, Cornu et al. (1999), who studied Amazonian ferralsols, found that Ti is mobile at a profile scale and cautioned against the use of Ti as a reference element. Interestingly, we find that relative to the parent gneisses, Ti is enriched in both saprolites and nodules, whereas Al is enriched in saprolite but depleted in the nodules. This indicates mobilization of both the elements in the present study area. It has been suggested that Ti content may increase with weathering, particularly in highly weathered rocks, because of chemical and or physical removal of other elements (Maynord, 1992; Young and Nesbitt, 1998). Sugitani et al. (1996) has reported high Ti/Al values in Archean cherts and suggested that it was due to Al loss at very low pH values.

From the mode of occurrence and chemical data, we suggest that, unlike their host saprolite, the nodules are not a residual product of weathering; they were likely formed because of mobilization and reprecipitation of Fe, Ti, and Mn as discrete secondary phases. Mn distribution within the nodules is discussed later. Goethite, hematite, anatase and titania (TiO_2) have been identified in the nodules from X-ray diffraction data. The mobilization and precipitation of Fe with the aluminous material produced by ferrolysis reaction could be responsible for the occurrence of kaolinite and gibbsite even for the low Al content in the nodules. Under hydromorphic conditions intense chemical weathering is probably biologically mediated and could mobilize Fe and Ti. For example, siderophore-produced organic acids can weather Ti-bearing minerals completely (Maurice et al., 2000; Schroeder et al., 2004). Schroeder et al. (2004) have suggested that incongruent weathering of biotite could also provide Ti during kaolinisation. We argue that whereas Ti could accumulate in the saprolite because of the loss of other elements, the same process could not account for the observed Ti enrichment in the nodules.

Saprolite and nodules contain much higher TiO_2 than the parent rocks, (0.2–0.6%, 0.3–1.6% and 0.1% TiO_2, respectively). This indicates that the excess Ti present in saprolites and nodules has been mobilized from a larger volume of parent rock than is represented by the present weathering profile. This inference is also supported by the enrichment of Ce in the saprolite and nodules, which is discussed later. We infer from the TiO_2 contents among parent rock, saprolites and Fe-nodules that Ti can be mobilized during weathering and concentrated within saprolites and nodules. The extent and mechanism of mobilization of Ti during rock weathering need to be further investigated in different physicochemical conditions to test the efficacy of using Ti as a provenance indicator and as a reference element in weathering studies.

4.3. Speciation analysis and redistribution of elements

Elements liberated during weathering become partitioned into different species in saprolites and soils. It is very difficult to identify mineral species because the crystal chemistry of nodule minerals that sequester elements from the soil solution is poorly understood (Manceau et al., 2003). Understanding the complex sorption behavior of elements, formation of different chemical species and association behavior of different elements, is very important in evaluating elemental mobility and redistribution process during different stages of chemical weathering and denudation. Therefore, we have tried, although indirectly, to identify some of the important phases in the nodules using a combination of speciation data and statistical analysis of elemental abundance.

Water soluble, exchangeable, amorphous, and crystalline Fe oxide species were separated from the nodules using the speciation protocol after Leleyter and Probst (1999), and were analyzed for their chemical constituents. The abundance of various elements in different fractions is plotted in Fig. 4. We found that Ti, Fe, Al, Cr, Ni, Mn, and Ba occur mainly in the crystalline and amorphous phases. Mg

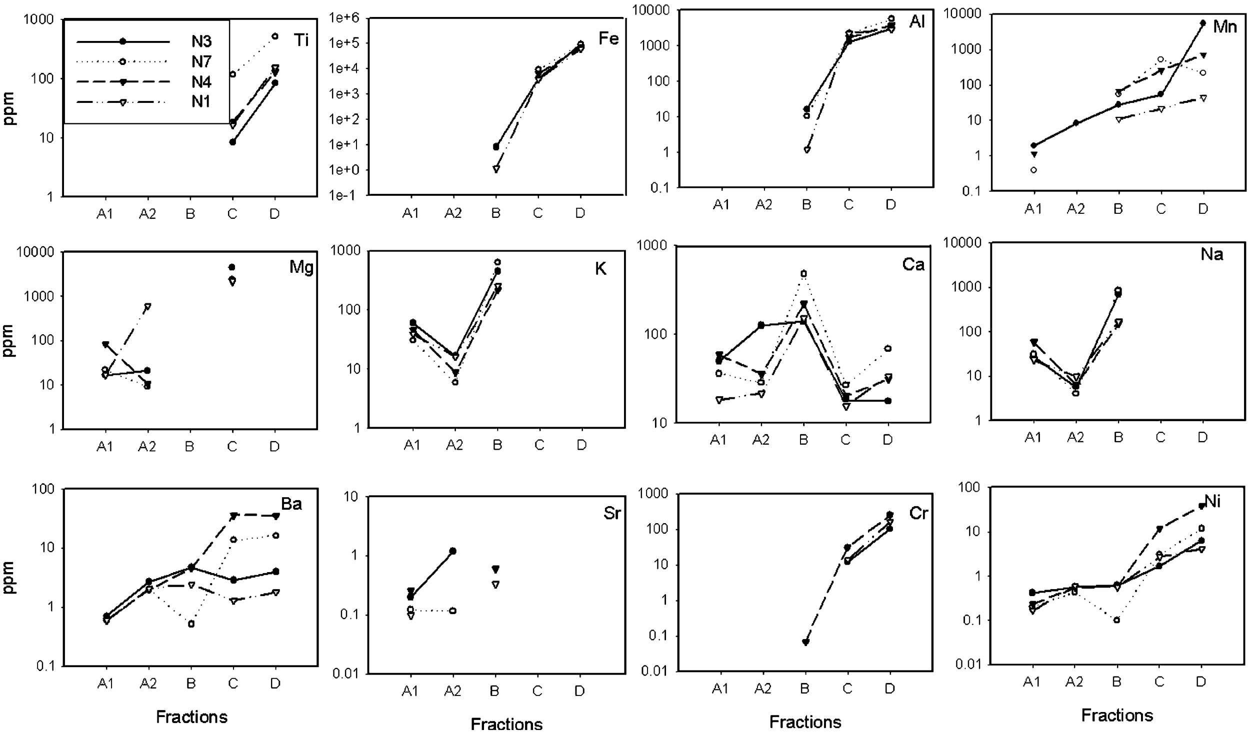

Fig. 4. Elemental concentration (ppm) of the different chemical fractions (A1 and A2-water soluble, B-exchangeable, C-amorphous and D-crystalline) of nodules is plotted on a log scale. Speciation shows that Ti, Fe, Al, Cr, Ni, Mn, and Ba occur mainly in the crystalline and amorphous phases. Bulk chemical data and speciation indicate that Fe and Al are the most important elements involved in the nodule formation and occur as crystalline and amorphous phases. Amorphous and crystalline phases are also important for Ti and Mn.

occurs mostly in amorphous phases. Ca and Sr occur in the soluble, exchangeable, and crystalline phases; Na and K, however, are concentrated only in the exchangeable fraction. Therefore, exchangeable forms are important for Ca, Na, K, and Sr. Bulk and speciation analyses indicate that Fe and Al are the most important elements involved in the making the nodules, and occur as crystalline and amorphous phases. Amorphous and crystalline phases are also important for Ti and Mn. X-ray diffraction data show the presence of goethite as the major mineral in the nodules. Ageing could be responsible for the transformation of amorphous phases (ferryhydrite) to the crystalline phases of goethite in the nodules (Yapp, 2001; Houben, 2003). Other important minerals present are kaolinite, gibbsite, anatase/titania, and quartz.

4.4. Statistics of the elemental distribution

Correlation coefficients (*r*) among the different elements analyzed were calculated for the samples of saprolites and nodules separately to understand the behavior of elements in the two different geochemical situations. Elements were mobilized from the weathering profile and concentrated in nodules within the profile at localized sites which acted as sinks for the mobilized elements. Although nodules were formed within the weathering profile, the geochemical conditions were likely different at the nodule forming centers. This may be attributed to several factors, such as (1) local microenvironmental conditions within the weathering profile (controlled by many physical properties including texture, porosity, permeability, and depth to the water table), (2) seasonal changes in precipitation, and (3) influence of microorganisms in response to 1 and 2. Therefore, we may have to consider the saprolites (as the source of elements for nodules) and nodules (elemental sinks) as two distinct geochemical products of weathering.

In the weathering profile, silica and alumina negatively correlate with other elements due to the dilution effect of Al and Si. Fe correlates with most of the elements in the weathering profile (Ti 0.99, Mn 0.76, Ca 0.85, P 0.94, Co 0.83, Cr 0.98, Ni 0.83, V 0.99, Zn 0.72, and REEs >0.84). Mn correlates with Mg (0.98), Ca (0.89), K (0.86), P (0.74), Co (0.99), Cr (0.76), Ni (0.89), V (0.8), Zn (0.99) and REEs (>0.90) except for Ce (0.75), Er (0.85), and Yb (0.71). This indicates that discrete Fe and Mn minerals play an important role in scavenging trace elements during saprolite formation (Manceau et al., 2003). V and P are strongly correlated (0.94) in the weathering profile, suggesting their coherence in biogeochemical systems. Local precipitation of vandate and phosphate ions can occur in the presence of hydroxides of aluminum and ferric iron. From the correlation matrix it appears that the REE are either associated with Fe–Ti bearing primary minerals or their secondary products. Correlation among Ca, P, and REE indicates that another phase of importance could be apatite/florencite.

In the nodules, only V and, to some extent, Cr shows positive correlation with Fe (0.92 and 0.57, respectively). Again Cr shows coherence with Al. Many trace elements are negatively correlated with Fe and Al, perhaps a likely dilution effect. A significant correlation of V and Cr with Fe indicates that these two trace elements geochemically behave in concert or they are taken up by the iron phases. Among all the transition metals Cr^{3+} is the most mimetic to Fe^{3+} (Manceau et al., 2000). Mn correlates well with Mg, Ca, K, Ba, Sr, Co, La, and Eu, showing the importance of discrete Mn phases in the nodules (discussed below). Ti also shows a very good correlation with Cr, Cu, and Ni. Mg, Ca, and K better correlate with the LREE than the HREE. Silica shows a positive correlation with REE but more so with the HREEs (Gd, Dy, Er, and Yb).

4.5. Chemical phases of the nodules

From the information obtained through speciation and mathematical correlation we infer that authigenic phases, most importantly the amorphous phases that are not readily identifiable by X-ray diffraction, have significant control in elemental redistribution during nodule formation. Speciation and bulk chemical analysis show that Fe, Al, and Mn, constituting the amorphous and crystalline phases, are important in the bulk chemistry of the nodules. We also infer that in the process of Fe nodule formation, Fe and Mn did not form solid solutions but likely precipitated as distinct phases (Manceau et al., 2000). Geochemical and mineralogical data suggest that goethite, gibbsite and kaolinite are the basic nodule building minerals. Although, XRD did not reveal the presence of any Mn mineral, the occurrence of Mn, Mg, Ca, and Ba together in the same extracted fraction, i.e., the amorphous phases liberated through speciation protocol, and the correlation of Mn with Mg, Ca, K, Ba, Sr, and Co, point to the presence of an amorphous Mn mineral in the nodules. This mineral can also explain the added 'CN' (Ca + Na) component in the A–CN–K diagram for the nodules. The potential minerals to exhibit such kind of compositional behavior are todorokite (Ca, Na, and $K)_{0.3-0.5}$ Mn(IV), Mn(III), $Mg)_6O_{12}$ 3–4.5 H_2O, and birnessite (Na, Ca, Mn(II), and $Mn_7O_{14}{\cdot}2.8H_2O$ (Post, 1999). These are commonly occurring terrestrial minerals in weathered zones and soils. They are also the major Mn minerals of oceanic Fe–Mn nodules. Tunnel and interlayer structures of these minerals can hold a wide range of cations. These minerals readily participate in a wide variety of oxidation and reduction and cation exchange reactions. A good correlation of Mn, Mg, and Ca with Ba, Sr, and Co clearly indicates that they are associated with this kind of Mn-mineral rather than adsorbed onto Fe oxide/oxyhydroxide (Fe has negative correlations with these elements).

The speciation and correlation analysis also indicated that whereas both Fe and Mn phases are important for the distribution of trace elements in the weathering profile, only the Mn phases in the nodules seem to scavenge the trace elements more significantly than Fe oxide phases. We suggest that the oxides and hydroxides of Fe and Mn, occurring as coatings on mineral surfaces in the saprolites, could scavenge trace elements by adsorption. Fe–Ti oxyhydroxides coating has been reported to be an important phase containing the REEs in sediments (Nesbitt, 1979; Middelburg et al., 1988; Singh and Rajamani, 2001). However, the crystalline phases of Fe in the nodules, e.g., goethite, may not be as efficient at scavenging the various elements as the Mn phases. This is because (1) Mn could form scavenging phases during Fe-nodule formation through mobilization of Mn from saprolites and (2) Mn phases have crystal structures, particularly tunnels and interlayers, suitable for the effective capture of trace elements. Also, the ageing and transformation of ferryhydrite to goethite may have resulted in the exclusion of some trace elements (Houben, 2003). The correlation values of Ti with Cu, Ni and Cr, occurrence of amorphous/crystalline Ti phases, and high Ti contents in the nodules, all suggest the importance of secondary Ti minerals for these trace elements in the nodules. How Ti controls the distribution of these trace elements in the saprolite and nodules requires detailed study.

4.6. Rare earth elements (REE) geochemistry

Thick weathering profiles have developed on migmatitic bedrocks with granitic leucosomes, biotite rich gneiss melanosomes, quartz veins, and with amphibolitic enclaves. The granitic matrix, which was converted to saprolite, has a low REE abundance, a fractionated pattern and a small positive Eu anomaly because of feldspar dominance. Biotite-rich melanosomes have similar REE patterns, but with much higher REE abundance, because of their more mafic chemistry with significantly higher Ti contents. Although chondrite-normalized REE patterns (Fig. 5a–c) show the behavior of REE during weathering, the parent rock-normalized REE patterns (Fig. 6a and b) are more informative for understanding the development of saprolite and nodules from sampling site-1. In Fig. 6a, saprolite samples show a strong enrichment in HREE with weathering, and depletion in LREE abundance (except for Ce). Weathering also resulted in the development of negative Eu and positive Ce anomalies in saprolite. A high degree of chemical weathering and destruction of Eu-bearing feldspars may have removed the positive Eu anomaly and may have even developed a negative Eu anomaly (Condie et al., 1995; Tripathi and Rajamani, 2003). The development of a positive Ce anomaly is likely redox controlled, as explained below. The behavior of LREE, HREE, Eu, and Ce indicates that most of the REE were mobilized during weathering but HREE were precipitated in the saprolite. We note that, whereas the LREE maintain their patterns in the saprolite, similar to that of the unweathered rock, the HREE show flattened patterns (in Fig. 5a and b) because of enrichment. The extent of enrichment for HREE increases with increasing atomic number (see Fig. 6a). This suggests that the HREE redistribution was controlled by atomic size and by the secondary minerals formed during weathering. The HREE enriched saprolite samples contain vermiculite, illite, chlorite, kaolinite, and Fe–Mn oxy-hydroxides. Nesbitt (1979) has reported that moderately weathered zones containing vermiculite, Fe oxides, relict biotite and subordinate kaolinite and illite might preferentially accommodate HREE, while kaolinite and illite-rich residual material could be LREE enriched. Coppin et al. (2002) has shown that kaolinites can also have HREE-enriched patterns.

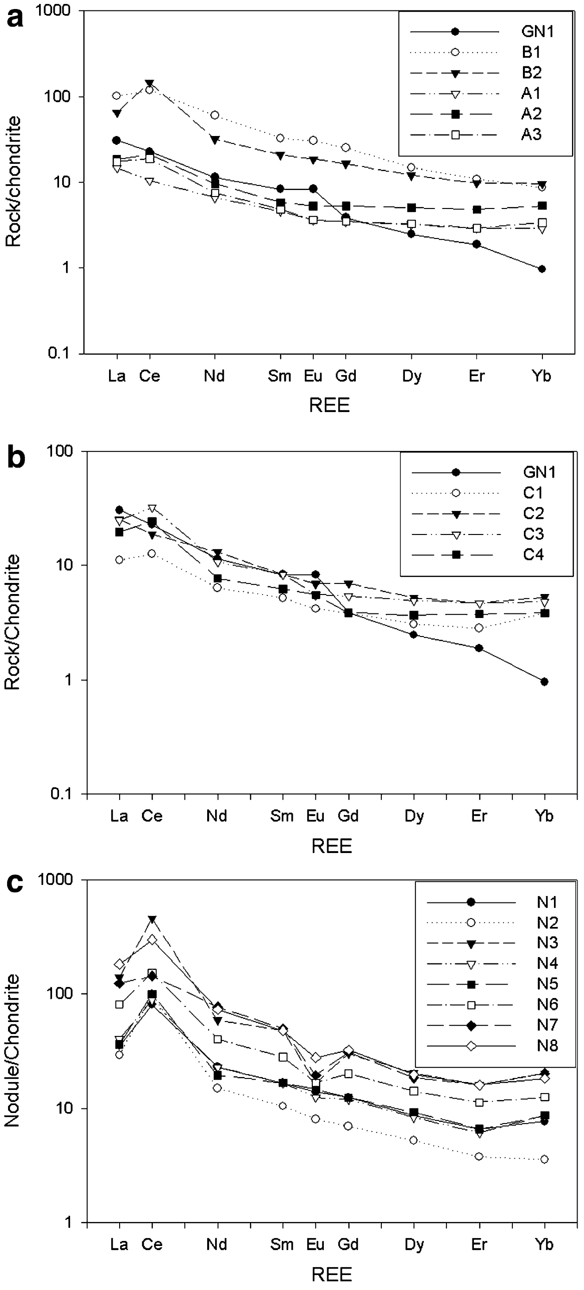

Fig. 5. Chondrite normalized REE patterns are shown for unweathered parent granodiorite gneiss (GN1), saprolites after granodiorite gneisses (A1–A3 and C1–C4) and biotite gneiss (B1–B2). With weathering, saprolites show enrichment in HREE and depletion in LREE abundance (except for Ce), all relative to fresh bedrock (a and b). Weathered saprolites, therefore, have flattened patterns. The nodules in the saprolites as well as from streambeds all have similar REE patterns but with variable abundance (c). All nodules have strong positive Ce anomalies, variable negative Eu anomalies, and HREE enrichment with respect to parent rock.

The nodules in the saprolites as well as from streambeds all have similar REE patterns but with variable abundance (Figs. 5c and 6b). All these nodules have strong positive Ce anomalies, higher REE abundance and variable negative Eu anomalies. Nodules developed over the Belur profile have lower REE abundance relative to those found on the streambeds, which could have formed from bedrocks

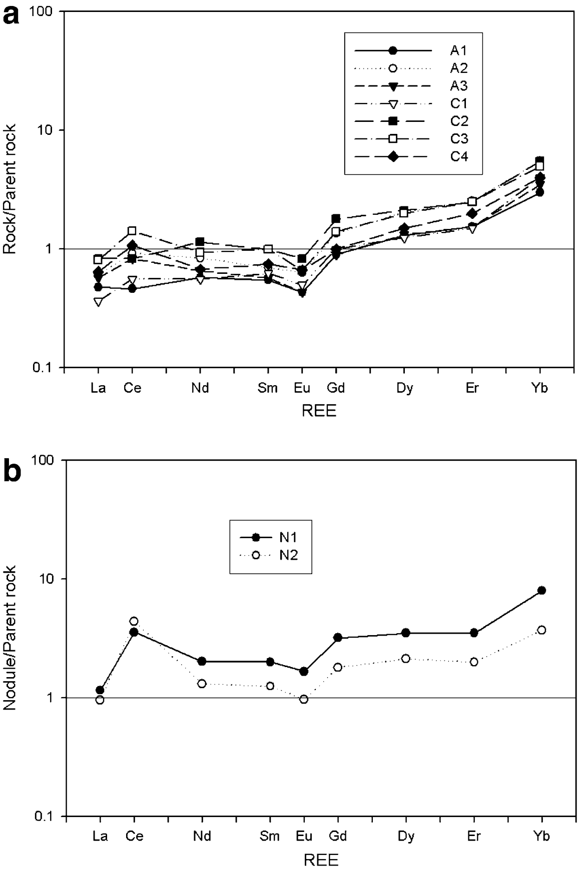

Fig. 6. Parent rock normalized REE patterns of the saprolites (a) and nodules (b), from the Belur profile. Note the enrichment of HREE in the saprolites and that all the REE in the nodules are in the order of Ce > HREE > LREE.

with variable REE abundance. Relative to their host saprolite, nodules are also slightly less fractionated, perhaps because of LREE enrichment, especially for Ce. This shows that Ce was decoupled from other LREE and likely was precipitated as discrete phases in the nodules, as discussed below.

In order to understand the redistribution of all elements during nodule forming processes, we also studied the correlation matrix for all analyzed elements. We note that REE correlate with various elements differentially, e.g., Si correlates relatively better with HREE, Mn with La and Eu, Mg with Nd, Sm and Eu, and Ca with Eu (see Appendix A). Therefore, the LREE seem to have been taken up by the Mn–Mg–Ca phase, which could be an amorphous Mn phase. However, in the weathering profile LREE correlate well with Ti, Fe, Mn, and P. This indicates that although the REE occur in the weathering profile, perhaps mainly in a few heavy mineral phases (e.g., Ti minerals, apatite, and florencite), in the nodules they may become redistributed among various secondary phases. This shows an evolving mineralogical control in REE redistribution during rock-weathering processes.

A good correlation of silica with HREE in the nodules is observed. This suggests co-precipitation of the mobilized HREE with secondary silica. The soils of the humid tropical Sahyadri region are acidic in nature (Bourgeon, 2001), and the A–CN–K and A–CNK–FM systematics of the nodules and saprolites also point to intensive chemical weathering under very acidic conditions maintained perhaps by high organic activity. Mobilization of Fe^{2+}, and ferrolysis weathering (Eqs. 1–4) of aluminosilicate minerals during nodule formation, occur only in acidic soil solutions. After breakdown the HREE-bearing 2:1 clays could provide HREE to the acidic solutions. Free silica is produced due to the disintegration of 2:1 and 1:1 clay precipitates in the acidic soil solutions. Nodules are known to contain secondary silica (Onac et al., 1997; Hlawatsch et al., 2002), and we also find silica/opal within the nodules. The silica precipitation could trap the REE from the acidic solution. It has been found that the sinters precipitating from low temperature hydrothermal fluids have REE patterns similar to that of the acidic hydrothermal fluids (Lewis et al., 1997). Götze (2001) found similarity in the REE chemistry of agate and parent volcanic rocks and suggested that the fluids circulating during alteration mobilized REE. However, how the REE get trapped and occur with silica are not well understood.

REE redistribution among various secondary phases during intense chemical weathering, Ce fractionation, and the origin of Ce positive anomaly in the nodules have important implications for the conditions of nodule genesis and the geochemical cycling of Ce between the continents and the ocean. Positive Ce anomaly in ferromanganese nodules and complementary negative anomaly in seawater were explained to result from oxidation of Ce(III) to CeO_2 in seawater, fractionation from other REE, and coprecipitation with the phases of Mn nodules (Goldberg et al., 1963). Initially, this phenomenon was described exclusively within ocean basins (de Baar et al., 1985). However, Ce anomalies in river waters (Elderfield et al., 1990; Sholkovitz, 1992), weathered rocks and lateritic profiles (Braun et al., 1990; Marsh, 1991) and nodules (Palumbo et al., 2001) have also been reported. How silicate weathering on continents affects seawater chemistry is not well understood. It has been suggested that oceanic nodules have a direct seawater source with respect to the REE (Glasby, 1973; Piper, 1974), whereas others suggest the possibility of sources from underlying ocean sediments (Bender, 1972). However, in a continental context, the source of REE could only be soil solutions formed by rock weathering. Highly acidic solution may leach the REE from minerals and transport them locally. Eu and Ce may be mobilized to a greater extent if they are in reduced forms (Eu^{2+} and Ce^{3+}). Continental nodules can be formed under humid conditions in the fine-grained saprolites by precipitation of metal ions locally. The atomic properties of Ce (Ce^{3+} and Ce^{4+}) govern its precipitation in the changed physicochemical conditions. It has also been suggested that preferential leaching of REE other than Ce could produce positive Ce anomaly in weathered rocks (Marsh, 1991), as also seen in the saprolites here. In the nodules, however, the sharp enrichment of Ce is a consequence of Ce mobilization and precipitation in the nodules. Enrichment of REE in the lower/inner weathering zones by supply from overlying saprolite has also been observed (Nesbitt and Markovics, 1997; Tripathi and Rajamani, 2003).

From the foregoing discussion, we suggest that an extensive column of weathered rocks existed in the past over the presently exposed weathering profile, and that these rocks have been removed by erosion. These weathered gneisses must have supplied REE to the nodules, just as they provided Ti to the saprolites and nodules. Amorphous phases of Mn, as well as all secondary phases of Fe–Ti that precipitated to make nodules, could have sequestered the LREE from the mobilized REE. Enrichment of Ce in saprolites and nodules, however, could have resulted from different processes of secondary mineral formation. In the nodules, Ce does not show any correlation with other elements present because it may occur as discrete phases as CeO_2 (Braun et al., 1990). In the saprolites, Fe, Ti, and Ce show a good correlation (see Appendix A) indicating their association with secondary Fe–Ti minerals. The observed coherence of Ce and Ti is likely because of similarity of their oxidation states, 4+ in both cases, in oxidizing soil water. Preferential retention of Ce with secondary phases of saprolites and more so of nodules could result in a significant depletion of Ce in the weathering solution or soil water. This may ultimately result in the observed negative Ce anomaly of river waters (Goldstein and Jacobsen, 1988; Elderfield et al., 1990; Sholkovitz, 1992; Ingri et al., 2000). These results on Ce anomalies and geochemical coupling of Ti and Ce in a continental setting demonstrate that these features are not only oceanic but also a continental phenomenon. Therefore, this geochemical coherence between these two elements will have implications to palaeoclimatic and provenance studies of ancient sediments. However, the mechanism of this process could be different in the ocean. Our work underscores that there is a greater need for detailed understanding of how (mechanism), and to what extent, continental weathering, lateritization and nodule genesis contribute to the ocean water Ce anomaly through river runoff.

5. CONCLUSIONS

From observations and discussions on weathering and formation of saprolites and nodules from granodiorite gneissic rocks in the Mysore Plateau, we conclude that:

1. Nodules represent a stage further in progressive chemical weathering under humid conditions (i.e., nodules formed from saprolite). The extensive weathering has facilitated nodule formation through ferrolysis-precipitation of goethite, ferrihydrite, hematite and gibbsite by reactions of Fe-bearing soil solutions with the aluminosilicate minerals. These reactions can take place only under hydromorphic conditions although the area presently is arid.
2. In the saprolites, enrichments of Al, Fe, and Ti, occur as residues, i.e., due to the removal of Si, Ca, Na, and K. In the nodules, enrichment of Fe, Ti, Cr, and Ni requires transport and deposition. Even Ti was mobilized, transported and deposited under the conditions of nodule formation.
3. In the nodules, Fe, Al, Ti, and Mn are the most important elements and occur as crystalline and amorphous phases. Mg occurs in amorphous phases, and Ca, Sr, Na, and K occur in exchangeable and soluble forms.
4. In the saprolites, trace elements are scavenged by Fe–Ti and Mn oxyhydroxides coatings whereas, in the nodules discrete amorphous Mn phases (e.g., todorokite) and Ti phases concentrate the trace elements.
5. REE were mobilized during weathering. In the saprolites, HREE were enriched because of secondary minerals (2:1 and 1:1 clays). In the nodules, LREE, particularly Ce, were further selectively concentrated, again because of precipitating minerals in the nodules. Ce retention in the nodules is so high that under similar conditions, soil and river water could be imparted with a negative Ce anomaly. To what extant continental weathering contributes to the negative Ce anomaly of ocean water is not known.
6. Under the conditions of saprolite and Fe nodule formation, Ti and Ce show a very similar geochemical enrichment.

ACKNOWLEDGMENTS

This research is supported by a grant from the Department of Science and Technology, Government of India to V.R. We are thankful to Meenal Mishra and Pankaj Mehta for discussion during fieldwork and help in the geochemical lab work. J.K.T. acknowledges Prof. B.R. Arora, Director, Wadia Institute of Himalayan Geology, India for his encouragement. We are very grateful to R. Byrne, Associate editor, G. Young and two anonymous reviewers for their thorough and helpful revision which improved the presentation of the manuscript.

APPENDIX A. SUPPLEMENTARY DATA

Supplementary data associated with this article can be found, in the online version, at doi:10.1016/j.gca.2007.01.001.

REFERENCES

Babu P. V. L. P. (1975) A study of cyclic erosion surfaces and sedimentary unconformities in the Cauvery basin-South India. *J. Geol. Soc. Ind.* **3**, 349–353.

Bau M., Koschinsky A., Dulski P., and Hein J. R. (1996) Comparison of the partitioning behaviours of yttrium, rare earth elements, and titanium between hydrogenetic marine ferromanganese crusts and seawater. *Geochim. Cosmochim. Acta* **60**, 1709–1725.

Bender M. L. (1972). Mechanisms of trace metals removal from the ocean. In *Ferromanganese Deposits on the Ocean Floor* (ed. D.R. Horn). National science Foundation, pp. 73– 80.

Bhaskar Rao Y. J., Naha K., Srinivasan R., and Gopalan K. (1991) Geology, geochemistry and geochronology of the Archean Peninsular Gneiss around Gorur, Hassan District, Karnataka, India. *Proc. Indian Acad. Sci. (Earth Planet. Sci.)* **100**, 399–412.

Bourgeon G. (2001) A survey of soils and weathering patterns through land system mapping in the western Ghats region. In Sahyadri: *The great escarpment of the Indian subcontinent* (eds. Y. Gunnel and B.P. Radhakrishna). Mem. Geol. Soc. India. pp. 855–904.

Braun J., Pagel M., Muller J., Bilong P., Michard A., and Guillet (1990) Cerium anomalies in lateritic profiles. *Geochim. Cosmochim. Acta* **54**, 781–795.

Burns R. G., and Burns V. M. (1975) Mechanism for nucleation and growth of manganese nodules. *Nature* **255**, 130–131.

Byrne R., and Sholkovitz E. (1996) Marine chemistry and geochemistry of lanthanides. In *Handbook on the Physics and Chemistry of the Rare Earths*, (eds. K. A. Gschneider Jr. and L. Eyring). Elsevier, Amsterdam, pp. 497–593.

Caner L., and Bourgeon G. (2001) On the possibilities of palaeoenvironmental reconstitution offered by tropical highland andisols. Example of Nilgiri andisols (South India). *C. R. Acad. Sci. Ser. IIA Earth Planet. Sci.* **333**, 725–731.

Condie K. C., Dengate J., and Cullers R. L. (1995) Behavior of rare earth elements in a palaeoweathering profile on granodiorite in the Front Range, Colorado, USA. *Geochim. Cosmochim. Acta* **59**, 279–294.

Coppin F., Berger G., Bauer A., Castet S., and Loubet M. (2002) Sorption of lanthanides on smectite and kaolinite. *Chem. Geol.* **182**, 57–67.

Cornu S., Lebon E., Ambrosi J. P., Luizao F., Rouiller J., Bonnay M., and Neal C. (1999) Evidence of titanium mobility in soil profiles, Manaus, Central Amazon. *Geoderma* **91**, 281–295.

Crerar D. A., and Barns H. L. (1974) Deposition of deep sea manganese nodules. *Geochim. Cosmochim. Acta* **38**, 279–300.

de Baar H. J. W., Bacon M. P., and Brewer P. G. (1985) Rare earth elements in the Pacific and Atlantic Oceans. *Geochim. Cosmochim. Acta* **49**, 1943–1959.

Dutta R. K., Acharya R., Nair G. C. A., Chintalapudi S. N., Chakravortty V., Reddy A. V. R., and Manohar S. B. (2005) Application of k_0-based INAA method in the studies of rare earth and other elements in manganese nodules from Indian Ocean. *J. Nucl. Radiochem. Sci.* **6**, 139–143.

Elderfield H., Upstill-Goddard R., and Sholkovitz E. R. (1990) The rare earth elements in rivers, estuaries, and coastal seas and their significance to the composition of ocean waters. *Geochim. Cosmochim. Acta* **54**, 971–991.

Elderfield H., Hawkesworth C. J., Greaves M. J., and Calvert S. E. (1981) Rare element geochemistry of oceanic ferromanganese nodules and associated sediments. *Geochim. Cosmochim. Acta* **45**, 513–528.

Gasparatos D., Haidouti C., and Tarenidis D. (2004) Characterization of iron oxides in Fe-rich concretions from an imperfectly drained Greek soil: a study by selective-dissolution techniques and X-ray diffraction. *Arch. Agronomy Soil Sci.* **50**, 485–493.

Glasby G. P. (1973) Mechanisms of enrichment of the rarer elements in marine manganese nodules. *Mar. Chem.* **1**, 105–125.

Goldberg E. D., Koide M., Schmitt R. A., and smith R. H. (1963) Rare earth distribution in the marine environment. *J. Geophys. Res.* **68**, 4209–4217.

Goldstein S. J., and Jacobsen S. B. (1988) Rare earth elements in river waters. *Earth Planet. Sci. Lett.* **89**, 35–47.

Götze J. (2001) Geochemistry of agates: a trace element and stable isotope study. *Chem. Geol.* **175**, 523–541.

Gunnel Y. (1988) Passive margin uplifts and their influence on climatic change and weathering patterns of tropical shield regions. *Global Planet. Change* **18**, 47–57.

Gunnel Y. (2001). Environmental changes in the Western Ghats during the quaternary. In *Sahyadri: The great escarpment of the Indian Subcontinent* (eds. Y. Gunnel and B. P. Radhakrishna). Mem. Geol. Soc. India, pp. 817–832.

Haley B. A., Klinkhammer G. P., and McManus J. (2004) Rare earth elements in pore waters of marine sediments. *Geochim. Cosmochim. Acta* **68**, 1265–1279.

Haley B. A., Klinkhammer G. P., and Mix A. C. (2005) Revisiting the rare earth elements in foraminiferal tests. *Earth Planet. Sci. Lett.* **239**, 79–97.

Haug G. H., Gunther D., Peterson L. C., Sigman D. M., Hughen K. A., and Aeschlimann B. (2003) Climate and the collapse of Maya civilization. *Science* **299**, 1731–1735.

Hlawatsch H., Garbe-Schonberg C. D., Lechtenberg F., Manceau N., Tamura N., Kulik D. A., and Kersten M. (2002) Trace metal fluxes to ferromanganese nodules from the Western Baltic Sea as a record for long-term environmental changes. *Chem. Geol.* **182**, 697–709.

Houben G. J. (2003) Iron oxide incrustations in wells, part 1: genesis, mineralogy and geochemistry. *Appl. Geochem.* **18**, 927–939.

Ingri J., Andersson P. S., Widerlund A., Ohlander B., Gustafsson O., and Land M. (2000) The Ce anomaly in river suspended matter: an indicator of hydrogeochemical processes in boreal catchment. *J. Conf. Abstr.* **5**, 540.

Leleyter L., and Probst J. L. (1999) A new sequential extraction procedure for the speciation of particulate trace elements in river sediments. *Int. J. Environ. Anal. Chem.* **73**, 109–128.

Lewis A. J., Palmer M. R., Sturchio N. C., and Kemp A. J. (1997) The rare earth element geochemistry of acid-sulphate and acid-sulphate-chloride geothermal systems from Yellowstone National Park, Wyoming, USA. *Geochim. Cosmochim. Acta* **61**, 695–706.

Manceau A., Schlegel M. L., Musso M., Sole V. A., Gauthier C., Petit P. E., and Trolard F. (2000) Crystal chemistry of trace elements in natural and synthetic goethite. *Geochim. Cosmochim. Acta* **64**, 3643–3661.

Manceau A., Tamura N., Celestre R. S., Macdowell A. A., Geoffroy A., Sposito G., and Padmote H. A. (2003) Molecular-scale speciation of Zn and Ni in soil ferromanganese nodules from loess soils of the Mississippi Basin. *Environ. Sci. Technol.* **37**, 75–80.

Marsh J. S. (1991) REE fractionation and Ce anomalies in weathered Karoo dolerite. *Chem. Geol.* **90**, 189–194.

Maurice P. A., Lee Y. J., and Hersman L. E. (2000) Dissolution of Al-substituted goethites by aerobic Pseudomonas mendocina var bacteria. *Geochim. Cosmochim. Acta* **68**, 1363–1374.

Maynord J. B. (1992) Chemistry of modern soil as a guide to interpreting Precambrian palaeosols. *J. Geol.* **100**, 279–289.

McLennan S. M. (1993) Weathering and global denudation. *J. Geol.* **101**, 295–303.

Middelburg J. J., Weijden C. H. V. D., and Woittiez J. R. W. (1988) Chemical processes affecting the mobility of major, minor and trace elements during weathering of granitic rocks. *Chem. Geol.* **68**, 253–273.

Nahon D. B. (1991) *Introduction to the Petrology of Soils and Chemical Weathering*. John Wiley, New York.

Nesbitt H. W., and Markovics G. (1997) Weathering of granodioritic crust, long-term storage of elements in weathering profiles, and petrogenesis of siliciclastic sediments. *Geochim. Cosmochim. Acta* **61**, 1653–1670.

Nesbitt H. W. (1979) Mobility and fractionation of rare earth elements during weathering of a granodiorite. *Nature* **279**, 206–210.

Nesbitt H. W., and Young G. M. (1989) Formation and digenesis of weathering profiles:. *J. Geol.* **98**, 801–822.

Onac B. P., Pedersen R. B., and Tysseland M. (1997) Presence of rare-earth elements in black ferromanganese coatings from Vantului cave (Romania). *J. Cave Karst Stud.* **59**, 128–131.

Palumbo B., Bellanca A., Neri R., and Roe M. J. (2001) Trace metal partitioning in Fe–Mn nodules from Sicilian soils, Italy. *Chem. Geol.* **173**, 257–269.

Pattan J. N., Rao Ch. M., Migdisov A. A., Colley S., Higgs N. C., and Demidenko L. (2001) Ferromanganese nodules and their associated sediments from the Central Indian Ocean Basin: rare earth element geochemistry. *Mar. Georesources Geotechnol.* **19**, 155–165.

Piper D. J. (1974) Rare earth elements in ferromanganese nodules and other marine phases. *Geochim. Cosmochim. Acta* **38**, 1007–1022.

Post J. E. (1999) Manganese oxide minerals: crystal structures and economic and environmental significance. *Proc. Natl. Acad. Sci. USA* **96**, 3447–3454.

Radhakrishna B. P. and Vaidyanadhan R. (1997). Geology of Karnataka, Geological Society of India, Bangalore.

Radhakrishna B. P. (1952) The Mysore Plateau: its structural and physiographic evolution. *Bull. Mysore Geologists Assoc.* **3**, 1–53.

Radhakrishna B. P. (1993) Neogene uplift and geomorphic rejuvenation of the India Peninsula. *Curr. Sci.* **64**, 787–793.

Rama Rao P., and Divakara Rao V. (1994) Origin of polyphase gneisses associated with the Krishnarajapet Greenstone belt, Dharwar Craton. *J. Geol. Soc. Ind.* **43**, 539–547.

Schroeder P. A., Pruett R. J., and Melear N. D. (2004) Crystal-chemical changes in an oxidative weathering front in a Georgia kaolin deposit. *Clays Clay Miner.* **52**, 211–220.

Schwertmann U., and Murad E. (1983) Effect of pH on the formation of goethite and hematite from ferryhydrite. *Clays Clay Miner.* **31**, 277–284.

Sharma A., and Rajamani V. (2000) Weathering of gneissic rocks in the upper reaches of Cauvery River, South India: implications to neotectonics of the region. *Chem. Geol.* **166**, 203–223.

Sharma A., and Rajamani V. (2001) Weathering of charnockites and sediment production in the catchment area of the Cauvery River, Southern India. *Sed. Geol.* **143**, 169–184.

Sholkovitz E. R. (1992) Chemical evolution of rare earth elements: fractionation between colloidal and solution phases of filtered river water. *Earth Planet. Sci. Lett.* **114**, 77–84.

Singh P., and Rajamani V. (2001) REE geochemistry of recent clastic sediments from the Kaveri floodplains, Southern India: implication to source area weathering and sedimentary processes. *Geochim. Cosmochim. Acta* **65**, 3093–3108.

Spilde M. N., Boston P. J., Schelble R. T., and Papike J. J. (2002). Mineral precipitation by Mn-oxidizing microbes: comparing natural and cultured Mn-minerals. *Lunar and Planetary Science Conference XXXIII*, Lunar Planet. Inst., Houston. #1090 (abstr.).

Stiles C. A., Mora C. I., and Driese S. G. (2001) Pedogenic iron-manganese nodules in Vertisols: a new proxy for paleoprecipitation. *Geology* **29**, 943–946.

Sugitani K., Horiuchi Y., Adachi M., and Sugisaki R. (1996) Anomalously low Al_2O_3/TiO_2 value for Archean cherts from the Pilabra block, Western Australia-possible evidence for the extensive chemical weathering on the early earth. *Precambrian Res.* **80**, 49–76.

Tripathi J. K., and Rajamani V. (1999) Geochemistry of the loessic sediments on Delhi ridge, Eastern Thar Desert, Rajasthan: implication for exogenic processes. *Chem. Geol.* **155**, 265–278.

Tripathi J. K., and Rajamani V. (2003) Geochemistry of Delhi quartzites: implications for the provenance and source area weathering. *J. Geol. Soc. Ind.* **62**, 215–226.

Yapp C. (2001) Rusty relics of earth history: Iron (III) oxides, isotopes and surficial environments. *Ann. Rev. Earth Planet. Sci.* **29**, 165–199.

Young G. M., and Nesbitt H. W. (1998) Processes controlling the distribution of Ti and Al in weath1ering profiles, siliciclastic sediments and sedimentary rocks. *J. Sed. Res.* **68**, 448–455.

Associate editor: Robert H. Byrne